World Academy of Science, Engineering and Technology
International Journal of Mechanical and Mechatronics Engineering
Vol:1, No:4, 2007

Flow Modeling and Runner Design Optimization in Turgo Water Turbines

John S. Anagnostopoulos, and Dimitrios E. Papantonis

Open Science Index, Mechanical and Mechatronics Engineering Vol:1, No:4, 2007 publications.waset.org/9499/pdf

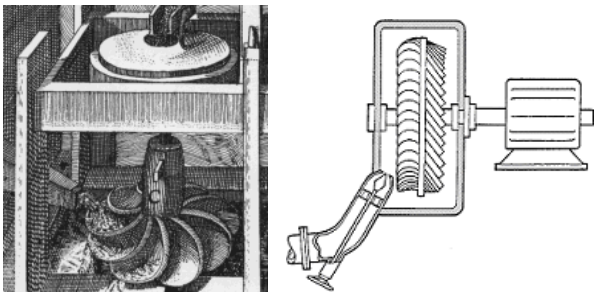
***Abstract*—**The incorporation of computational fluid dynamics in the design of modern hydraulic turbines appears to be necessary in order to improve their efficiency and cost-effectiveness beyond the traditional design practices. A numerical optimization methodology is developed and applied in the present work to a Turgo water turbine. The fluid is simulated by a Lagrangian mesh-free approach that can provide detailed information on the energy transfer and enhance the understanding of the complex, unsteady flow field, at very small computing cost. The runner blades are initially shaped according to hydrodynamics theory, and parameterized using Bezier polynomials and interpolation techniques. The use of a limited number of free design variables allows for various modifications of the standard blade shape, while stochastic optimization using evolutionary algorithms is implemented to find the best blade that maximizes the attainable hydraulic efficiency of the runner. The obtained optimal runner design achieves considerably higher efficiency than the standard one, and its numerically predicted performance is comparable to a real Turgo turbine, verifying the reliability and the prospects of the new methodology.

***Keywords*—**Turgo turbine, Lagrangian flow modeling, Surface parameterization, Design optimization, Evolutionary algorithms.

I. Introduction

TURGO water turbines belong to the impulse type hydraulic machines along with the more common, Pelton turbines. Turgo turbines are well suited to replacing low head multi-jet Pelton or high head Francis turbines with poor part load efficiencies, and they can be used in medium to high heads, from 15 to 300 m. Like Pelton, Turgo turbine has a flat efficiency curve and provides excellent part-load efficiencies hence it constitutes the best solution for large flow rate variations. Also, it can operate for long periods and minimum wear when the water is laden with slit and other entrained matter.

The Turgo turbine was first patented by a European company in 1919, although the earliest design dates back to the end of the sixteenth century (Fig. 1a). The water jet enters one side of the runner and exits through the other (Fig. 1b). This allows for a more efficient escape of 'used' water, which does not interfere with the incoming jet. Hence, larger jet and flow rates can be treated compared to a Pelton runner of same diameter. As a result, a Turgo turbine has higher specific speed and smaller size than a Pelton turbine for the same power. This compensates for its more complex design and more difficult manufacturing process. Moreover, the smaller runner diameter allows to obtain a higher angular velocity, so that the turns multiplier in the coupling with the electrical generator can be avoided, decreasing the costs and increasing the mechanical reliability of the system.



(a) (b)

Fig. 1 (a) Earliest design of Giovanni Branca (b) Sketch of the Turgo type design

Very few scientific articles can be found in the literature dealing with the design of Turgo runner, and only few companies construct this turbine type worldwide. In most books and manuals that include impulse turbines description the Turgo turbine is referred simply as a variant of the Pelton turbine. An extended description is first given in Gibson [1], but without any information about dimensioning and design of the runner. Some interesting elements for dimensioning and standardization of small Turgo turbines are given in the manuals of Gaorong [2], [3], as well as by Bednar [4].

The numerical modeling and analysis of the flow in a Turgo runner, along with a preliminary design optimization study of its blades, is the aim of the present work. To achieve this, the inner surface of a blade is initially designed according to hydrodynamics theory and using Bezier polynomials, while a mesh-free Lagrangian method is adopted for the simulation of the free-surface flow developed on the blade surface. In order to improve the hydraulic efficiency of the initial design, a

Manuscript received July 23, 2007. This work is co-funded by the European Social Fund (75%) and National Resources (25%) – Operational Program for Educational and Vocational Training II, and particularly the Program Pythagoras.

J. S. Anagnostopoulos, Assistant Professor, is with the School of Mechanical Engineering, National Technical University of Athens, Greece (corresponding author, tel.: 210-7721080; fax: 210-7721057; e-mail: j.anagno@fluid.mech.ntua.gr).

D. E. Papantonis, Professor, is with the School of Mechanical Engineering, National Technical University of Athens, Greece (e-mail: papan@fluid.mech.ntua.gr).

Open Science Index, Mechanical and Mechatronics Engineering Vol:1, No:4, 2007 publications.waset.org/9499/pdf

stochastic optimization software based on evolutionary algorithms is implemented and a number of blade design parameters are considered and varied within certain limits. The main dimensions of the examined runner, as well as its nominal operation conditions, correspond to a real Turgo turbine installed in a small hydro power plant in Greece.

II. Runner Design & Parameterization

The mean velocity of the free jet emerging from the nozzle of the turbine is determined from the net head, by the equation [5]:

$$c = \varphi \cdot \sqrt{2\,g\,H} \approx 0{,}97 \cdot \sqrt{2\,g\,H} \tag{1}$$

where φ is the efficiency of the nozzle, taken here equal to 0,97. The corresponding jet diameter, d, can be obtained from the nominal flow rate:

$$Q_K = \frac{\pi}{4} \cdot d^2 c \tag{2}$$

At the best efficiency point the circumferential speed of the runner is connected with the jet velocity via the relation [5]:

$$u_1 \approx (0{,}46 - 0{,}47) \cdot c \tag{3}$$

Hence the diameter of the runner is (Fig. 2a):

$$D_s = \frac{60\,u_1}{\pi\,n} \tag{4}$$

where n is the runner speed in rpm.

The runner has a conical shape in the meridian plane (Fig. 2a). The inlet blade edge is a straight line and the inlet width is larger than the jet diameter ($b_1 = 1{,}2\ d$), in order to secure the entrance of the entire jet even for the highest flow rate. The runner width in the axial direction is taken $B \approx 1{,}45\ d$, and the outlet edge of the blade is drawn with the aid of a Bezier curve (Fig. 2a). The blade traces on the hub and the shroud are also generated using corresponding Bezier polynomials.

The blade inlet and outlet angles, β_1 and β_2, can be computed from the corresponding velocity triangles (Fig. 2b). At a given radial distance r, the runner peripheral velocity is: $u_1 = 2\pi nr$, whereas the absolute inlet flow velocity $c_1 = c$, and its angle relative to the runner disk is: $\alpha_1 = 25$ deg, for the examined turbine. At the best efficiency point the flow exits with zero circumferential velocity, hence the outlet velocity triangle is orthogonal and can also be constructed (Fig. 2b).

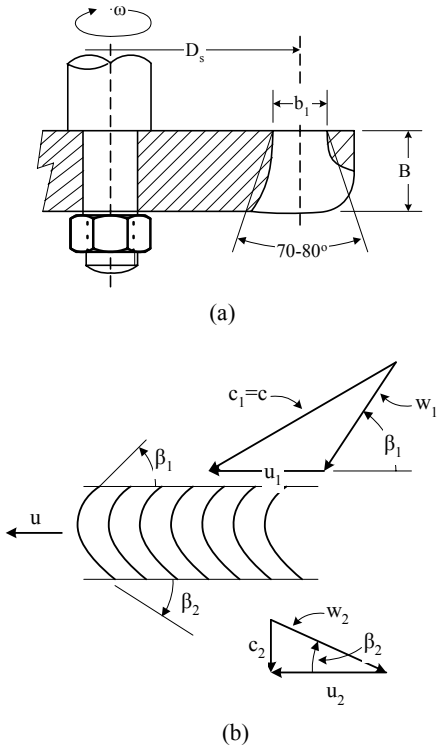


Fig. 2 Turgo runner configuration:
(a) Meridian plane (b) Velocity triangles

The mean 3-dimensional surface of the blade is then generated using the conformal mapping methodology in a number of meridian streamlines, and assuming a linear variation of the blade angle from the leading to the trailing edge. An example of the resulting shape is shown in Fig. 3. The leading edge line is represented by a parabolic function and has adjustable curvature (Fig. 3).

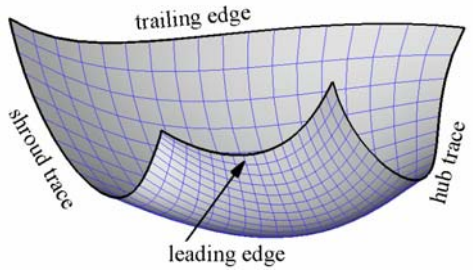


Fig. 3 Indicative view of mean blade surface

Next, the inner and outer surfaces of the blade are constructed considering a given blade thickness distribution, assumed here constant (Fig. 4). The leading edge is rounded to a semi-elliptic shape.

Finally, the hub and the shroud are easily introduced as axisymmetric surfaces, and the entire runner can be reproduced as shown in Fig. 5.

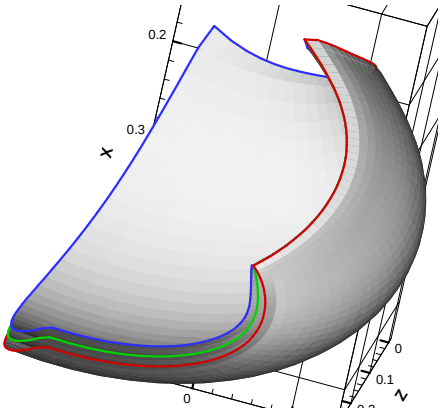


Fig. 4 Indicative Turgo blade shape

Modifications to the standard blade design can be made by introducing a number of additional design variables that permit the deviation from the standard blade inlet and outlet angles, as well as by applying a quadratic instead of a linear variation of the blade angle along a meridian stream line. Three corresponding parameters are used for each one of three different meridian lines (at the hub, shroud and one intermediate), giving, along with the leading and trailing edges control points, a total number of 11 free design variables. The rest lines of the blade surface are computed by interpolation techniques.

III. Flow Modeling

The free-surface flow in the rotating runner of an impulse turbine is complex and unsteady hence its simulation constitutes a difficult computational task. Thanks to the great progress in computing power since the graphical method of Brekke [6], the two-phase flow equations can now be solved using modern CFD tools [7]–[9]. The computer cost of these methods is however quite high, whereas some uncertainties concerning the jet flow at the nozzle exit and at the blade inlet, as well as some inaccuracies associated with the turbulence modeling, cannot be avoided. For this reason an alternative fast simulation methodology was developed and used for a Pelton runner with encouraging results [10], [11]. The methodology is based on the Lagrangian particle tracking approach, and although it cannot compete with the advanced Eulerian models in terms of nominal accuracy, its computer cost is practically negligible. Also, the method can provide details not only for the flow field, but also for the energy transfer in the runner.

In the Lagrangian formulation the fluid is represented by a statistically adequate number of fluid particles, the trajectories of which are computed by integrating their motion equations along the blade inner surface. Additional terms are introduced in these equations to account for the hydraulic losses, which were regulated in a previous work [10]. Minor hydraulic losses, losses due to changes in flow direction, as well as impact losses when a fluid particle impinges on the blade are considered, whereas gravity and pressure forces are neglected.

The starting points of the particles are uniformly distributed within the jet volume, and the time integration starts when the first particle of the jet impacts on a reference blade. Due to the rotation of the runner, the rest particles impact at different time instants and with different relative angles and velocities (Fig. 6).

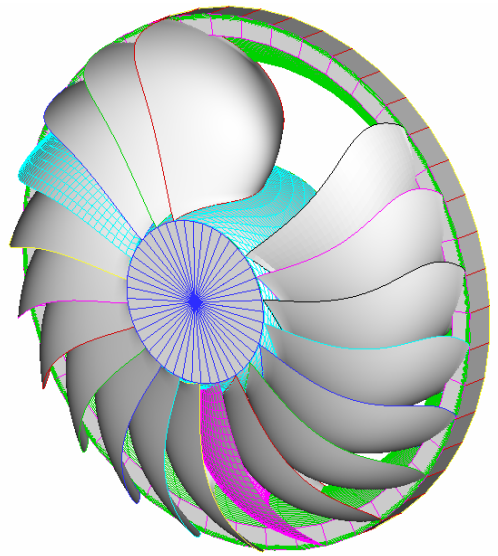


Fig. 5 Runner drawn with the present method

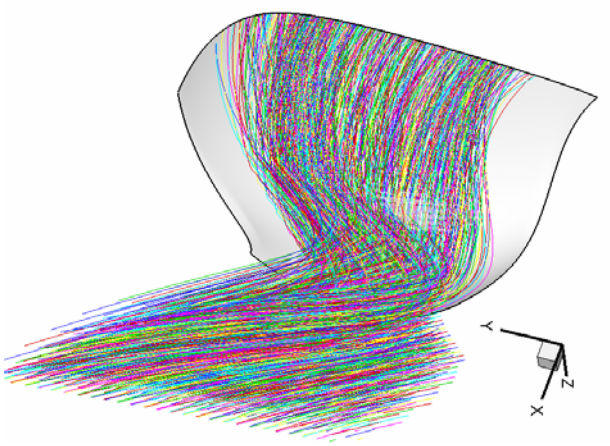


Fig. 6 Indicative particle trajectories (rotating system of reference)

The particle equations are solved by a second-order, predictor-corrector scheme in the rotating system of reference, using a sufficiently small time-step ($2x10^{-5}$ sec) to produce independent results. The particle path along the blade surface is computed at each time step from its velocity vector and the known local surface slope, and the trajectory is terminated when the particle flows out of the blade. Also, a particle is not counted in case that it passes by the reference blade or impinges on the next coming blade. A number of the about 10^3 fluid particles were found adequate to produce

Open Science Index, Mechanical and Mechatronics Engineering Vol:1, No:4, 2007 publications.waset.org/9499/pdf

Open Science Index, Mechanical and Mechatronics Engineering Vol:1, No:4, 2007 publications.waset.org/9499/pdf

independent results for the hydraulic efficiency of the runner, whereas for the reproduction of the surface flow pattern an order of magnitude more particles are tracked.

The mechanical torque M_{num} on the runner shaft is computed from the conservation of momentum:

$$M_{num} = \rho Q_u \cdot \left(\overline{r_{in}\, w_{in}} - \overline{r_{out}\, w_{out}} \right) \tag{5}$$

where Q_u is the cumulative flow rate that enters each blade. The mean angular momentum at the inlet, assuming a uniform, constant speed jet flow, becomes:

$$\overline{r_{in}\, w_{in}} \cong R_{j-r}\, V_{jet} \cos\varphi_{jet} \tag{6}$$

where V_{jet} is the mean jet flow velocity, $R_{j\text{-}r}$ is the normal distance between the jet and the runner axis and φ_{jet} is the jet inlet angle relative to the runner disk. The mean angular momentum at the blade outlet is computed by averaging the local fluid particle properties there:

$$\overline{r_{out}\, w_{out}} \cong \frac{1}{N} \cdot \sum_i y_{out,i} w_{out,i} \tag{7}$$

where $y_{out,i}$ and $w_{out,i}$ are the radial distance and the relative tangential velocity component, respectively, of a particle i at the moment it flows out of the blade, and N is the total number of fluid particles that impinge on the inner blade surface. The overall hydraulic efficiency of the runner is obtained as the ratio of the developed mechanical power on the shaft, divided by the corresponding net hydraulic power provided at the inlet:

$$\eta_h = \frac{M_{num}\, \omega}{\rho\, g\, Q\, H} \tag{8}$$

where H is the net hydraulic head, ω is the angular rotation speed of the runner and Q the jet flow rate. Notice that the runner flow rate Q_u in (2) may be less than Q for certain off-design operation conditions.

The main dimensions of the Turgo turbine examined here correspond to a real 1 MW machine operating in 'Kastaniotiko' small hydropower plant in Greece, whereas the standard blade design is obtained by the hydrodynamic analysis in chapter II. A post-processing algorithm is developed to facilitate the analysis of the numerical results. The detailed depiction of the flow field at every time instant and the flow animation can provide valuable and comprehensive information about the unsteady flow development and the energy transfer in the runner.

Some indicative pictures from the turbine examined here are illustrated in Fig. 7. The free-surface flow on a blade starts, evolves and terminates within about 110° of runner rotation. Soon after its impact on the reference blade (Fig. 7a), the jet starts to interact with the next coming blade too (not shown in Fig. 7), which eventually cuts the jet (Fig. 7c). A remarkable behaviour that can be observed is that the fluid leaves the blade from quite different regions during the interaction period (Figs. 7b,c,d), because of the blade elevation due to rotation. Therefore the correct design of the entire trailing edge line is decisive in order to achieve high efficiency.

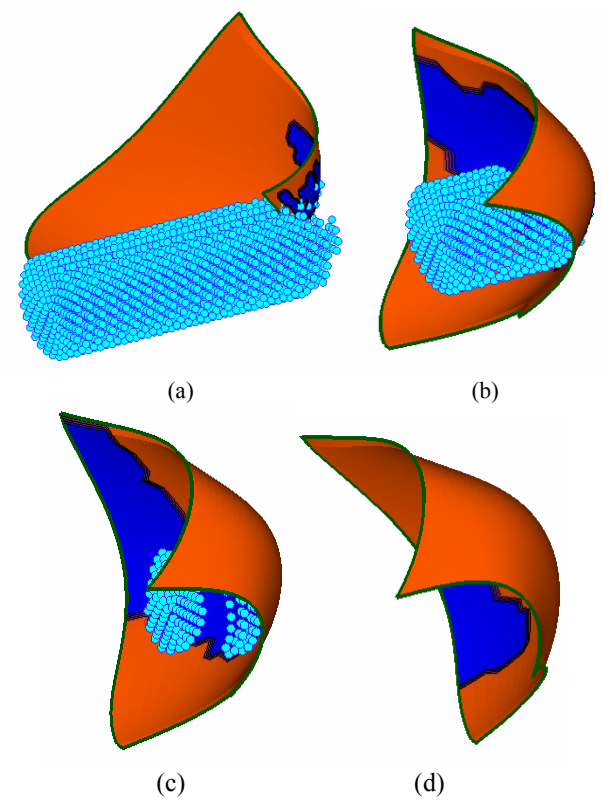


Fig. 7 Selected flow pictures: a) initial jet-blade interaction; b) full jet impingement; c) end of jet impingement; d) clearance phase

A large number of computer runs is performed in order to create the diagram of Fig. 8, giving the total efficiency of the runner in the entire operation range for one of the two jets in operation. The total efficiency is computed from (8), minus 3%, which is a reasonable estimation of the mechanical losses for the present turbine. The corresponding curves of the turbine manufacturer are plotted for comparison in Fig. 9. Although the qualitative view of Fig. 8 is reasonable, it can be observed that the predicted efficiency of the standard design maximizes at quite higher net head values (about 70 m, Fig. 8) compared to the nominal head of 55 m (Fig. 9). Moreover, the 80,8% maximum efficiency is remarkably lower than that of the real turbine (above 84%), and the difference becomes even higher at the design point (600 lt/sec – 55 m), where the standard runner's efficiency is only 78,5% (Fig. 8). An explanation for the discrepancy is that, due to the rotating motion of the blade, the relative inlet angle of the jet does not

Open Science Index, Mechanical and Mechatronics Engineering Vol:1, No:4, 2007 publications.waset.org/9499/pdf

remain constant and equal to the blade angle β_1 during the jet-runner interaction.

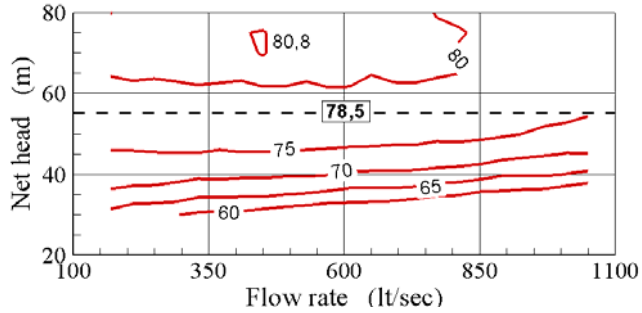


Fig. 8 Efficiency (%) chart of the standard design

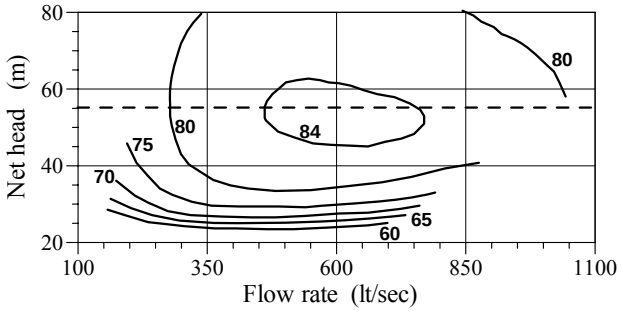


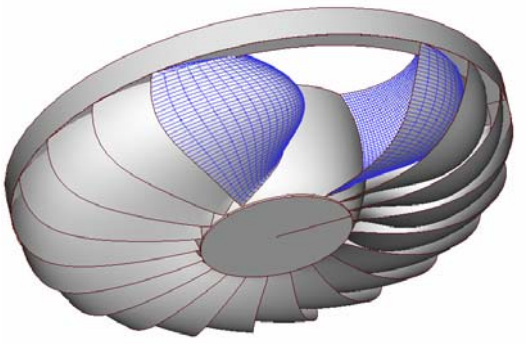
Fig. 9 Efficiency (%) chart of the real turbine

IV. Optimum Runner Design

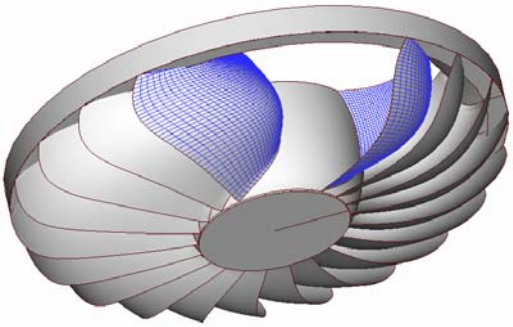
The general optimization software EASY, developed and brought to market by the Lab of Thermal Turbomachinery NTUA [12], is used in the present work to find the blade shape that achieves maximum hydraulic efficiency. The optimizer is based on evolutionary algorithms and it is suitable for complex non-linear and multi-parametric problems, as the shape optimization of a complex 3D surface. During an iterative process the optimizer selects values of the free design parameters from their prescribed ranges, and looks automatically for the set that maximizes the cost function (here the efficiency), using populations of candidate solutions instead of a single solution. To create the next generation the algorithm mimics the biological evolution of species generations, using processes like cross-over and mutation [12]. A number of about 10^3 evaluations (flow field simulations) were found adequate for convergence in the examined case, where 11 design parameters are used (chapter II).

As can be observed in the comparative view of Fig. 10, the obtained optimal runner exhibits noticeable differences from the standard one, since the modified inlet and outlet angles affect the entire surface shape and curvature of the blades.

On the other hand, the performance results show that the improved runner design achieves 6% higher efficiency than the standard one at the design point, whereas its efficiency diagram drawn in Fig. 11 agrees well with the manufacturer curves (Fig. 9), at least for high loads, above 500 lt/sec.



(a)



(b)

Fig. 10 Comparison between the standard (a), and the optimal runner (b)

As shown in Fig. 9, the attainable efficiency of the real turbine drops for flow rates below 500 lt/sec. This is mainly due to the inability of the valve to keep producing a totally smooth and axisymmetric jet, which may also start to decline from its main axis. Moreover, the smaller jet diameter is associated with greater percentage losses at its impact on the blade leading edge. The above mechanisms are however not modeled here, and for this reason the predicted efficiency in Fig. 11 remains constant or even slightly increases as the flow rate reduces, in accordance with the theory.

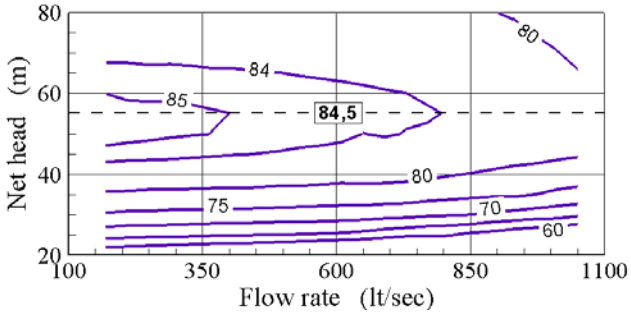


Fig. 11 Total efficiency of the optimal design

Open Science Index, Mechanical and Mechatronics Engineering Vol:1, No:4, 2007 publications.waset.org/9499/pdf

V. Conclusion

An effective and fast computational methodology based on the Lagrangian approach is developed and applied for the simulation and detailed analysis of the complex, unsteady, free-surface flow that evolves in the runner of a Turgo turbine. A standard runner design created by applying the hydrodynamics theory was found to be reasonable in shape and performance but not very efficient, while its best efficiency point is far from the desired operating conditions.

The blade geometry is parameterized using 11 design variables, and the combination of their values that maximizes the hydraulic efficiency of the runner is found using a powerful, stochastic optimization tool. The obtained improved runner exhibits remarkably higher efficiency than the standard design, and its characteristic curves are close to the corresponding ones of a real Turgo turbine.

A more elaborate modeling of the free-surface flow in the blades and of the jet structure at some complex regions is required to develop further the present numerical design optimization methodology, which appears to be very promising in order to improve the design process and the cost-effectiveness of this water turbine.

References

[1] A.H. Gibson, *Hydraulics and its application*s. Constable & Co Ltd, UK, 1952.

[2] L. Gaorong, *Small Hydro Power in China, Experience and Technology*. Hangzhou Regional Center for Small Hydro Power, Hangzhou, 1996.

[3] L. Gaorong, *A Manual of China Small-Hydraulic Turbine-Generating Units*. Hangzhou Regional Center for Small Hydro Power, Hangzhou, 1997.

[4] J. Bednar, *Turbiny*. SNTL Nakladatelstvi Technicke Literatury, Praha, 1989.

[5] M. Nechleba, *Hydraulic Turbines*. *Their Design and Equipment*. ARTIA, Prague, 1957.

[6] H. Brekke, *A general study on the design of vertical Pelton turbines*. Turboinstitut, Ljubljana, rep. No/46/3/Ada, 1984.

[7] S. Kvicinsky, F. Longatte, F. Avellan, and J.-L. Kueny, "Free surface flows: Experimental validation of the Volume of Fluid (VOF) method in the plane wall case," *Proceedings, 3rd ASME/JSME Conference*, San Francisco, ASME, N.Y., 1998.

[8] A. Perrig, M. Farhat, F. Avellan, E. Parkinson, H. Garcin, C. Bissel, M. Valle, and J. Favre, "Numerical flow analysis in a Pelton turbine bucket, *Proceedings,*" *22nd IAHR Symposium on Hydraulic Machinery and Systems*, June 29 – July 2, Stockholm, Sweden, 2004.

[9] A. Perrig, F. Avellan, J.-L. Kueny, M. Farhat, and E. Parkinson, "Flow in a Pelton turbine bucket: Numerical and experimental investigations," *ASME Trans., Journal of Fluids Engineering*, Vol. 128, 2006, pp. 350-358.

[10] J. Anagnostopoulos, and D. Papantonis, "Experimental and numerical studies on runner design of Pelton turbines," *Hydroenergia 2006*, 7-9 June, Crieff, Scotland, UK, 2006.

[11] J. Anagnostopoulos, and D. Papantonis, "A numerical methodology for design optimization of Pelton turbine runners," *HYDRO 2006*, 25-27 September, Porto Carras, Greece, 2006.

[12] K.C. Giannakoglou, "Design of optimal aerodynamic shapes using stochastic optimization methods and computational intelligence," *Progress in Aerospace Science*, Vol. 38, 2002, pp. 43-76.